Spectrochimica Acta Part A: Molecular and Biomolecular Spectroscopy 141 (2015) 104–112

Contents lists available at ScienceDirect

Spectrochimica Acta Part A: Molecular and Biomolecular Spectroscopy

journal homepage: www.elsevier.com/locate/saa

Spectroscopic investigations, molecular interactions, and molecular docking studies on the potential inhibitor "thiophene-2-carboxylicacid"

T. Karthick [a], V. Balachandran [b,*], S. Perumal [c]

[a] Department of Physics, K S R Institute for Engineering and Technology, Tiruchengode 637215, India
[b] Centre for Research, Department of Physics, A.A. Govt. Arts College, Musiri, Tiruchirappalli 621211, India
[c] PG & Research Department of Physics, S.T. Hindu College, Nagarcoil 629002, India

HIGHLIGHTS

- Vibrational FT-IR spectrum has been recorded and compared with simulated spectra.
- Charge transfer characteristics are analyzed by natural atomic orbital occupancies.
- Existence of dimer through carboxylic acid is discussed by NBO analysis.
- UV–Vis spectra of TCA in different solvents were simulated theoretically.
- The inhibition activities of TCA against 1CX2 and 1PTH have been discussed.

GRAPHICAL ABSTRACT

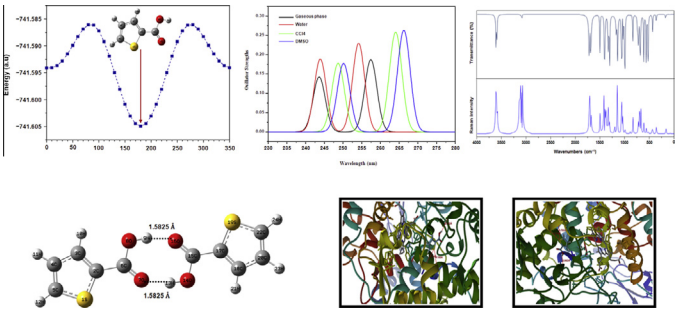

ARTICLE INFO

Article history:
Received 9 November 2014
Received in revised form 11 January 2015
Accepted 15 January 2015
Available online 2 February 2015

Keywords:
Thiophene-2-carboxylicacid
PES scan
FT-IR
NBO analysis
Molecular docking
Binding affinity

ABSTRACT

Thiophene derivatives have been focused in the past decades due to their remarkable biological and pharmacological activities. In connection with that the conformational stability, spectroscopic characterization, molecular (inter- and intra-) interactions, and molecular docking studies on thiophene-2-carboxylicacid have been performed in this work by experimental FT-IR and theoretical quantum chemical computations. Experimentally recorded FT-IR spectrum in the region 4000–400 cm^{-1} has been compared with the scaled theoretical spectrum and the spectral peaks have been assigned on the basis of potential energy distribution results obtained from MOLVIB program package. The conformational stability of monomer and dimer conformers has been examined. The presence of inter- and intramolecular interactions in the monomer and dimer conformers have been explained by natural bond orbital analysis. The UV–Vis spectra of the sample in different solvents have been simulated and solvent effects were predicted by polarisable continuum model with TD-DFT/B3LYP/6-31+G(d,p) method. To test the biological activity of the sample, molecular docking (ligand–protein) simulations have been performed using SWISSDOCK web server. The full fitness (FF) score and binding affinity values revealed that thiophene-2-carboxylicacid can act as potential inhibitor against inflammation.

Introduction

In the last two decades, several thiophene derivatives were studied by researchers in the spectroscopic and medicinal field due to their remarkable pharmacological and biological activities.

* Corresponding author. Tel.: +91 431 2591338; fax: +91 4326 262630.
E-mail address: brsbala@rediffmail.com (V. Balachandran).

http://dx.doi.org/10.1016/j.saa.2015.01.025
1386-1425/

Generally, they are being used as a chemical intermediate for the preparation of drugs, dyes and aroma compounds [1,2]. In particular, a title molecule thiophene-2-carboxylicacid (abbreviated as TCA) was reported as potential inhibitors of HCV NS58 polymerase and HCV subgenomic RNA replication [3,4]. Moreover, TCA molecule exhibit antiporphyric activity in allylisopropylacetamide treated animals [5]. The inhibition activity of Carbazolothiophene-2-carboxylic acid derivatives against endothelin-1 has been reported by Babu et al. [6]. Inhibition of endothelin-1 prevents pulmonary vasculature constriction and thus decreases pulmonary vascular resistance. Deng et al. reported Thieno[3,2-b]thiophene-2-carboxylic acid derivatives as GPR35 agonists [7]. GPR35 is an inhibitor drug used for treatment of Parkinson's disease, inflammation, pain, cardiovascular diseases, and metabolic disorders [8,9].

Due to their high impact in the medicinal field, certain thiophene derivatives have been studied earlier [10–19]. The scaled quantum chemical force filed calculations and vibrational spectra of liquid thiophene and methyl substituted thiophene derivatives have been studied by Pasterny et al. and Hernández et al. [10,11], respectively. Theoretical DFT, experimental Raman and NMR studies on thiophene, 3-methylthiophene and selenophene have been performed by Kupka et al. [12]. The conformational stability and normal coordinate analysis of thiophene-2-aldehyde were investigated by Fleming et al. [13]. Singh et al. investigated solvation effects of thiophene in two different polar solvents and also performed vibrational assignments in both experimental and theoretical aspects [14]. Vibrational spectroscopic characterization of 2-Dicyanovinyl-5-(4-N,N-dimethylaminophenyl) thiophene has been studied by Hong et al. [15]. Recently, the spectroscopic investigation of thiophene-2-carbohydrazide and N′-(Adamantan-2-ylidene)thiophene-2-carbohydrazide have been reported [16,17]. The enzyme inhibition activity of organotin (IV) derivatives of thiophene-2-carboxylic acid has been evaluated by Abbas et al. [18]. The molecular docking studies along with antimicrobial evaluation of thiophene bearing sulfisoxazole moiety have been performed by Nasr et al. [19]. The tentative assignment without detailed interpretation of FT-Raman spectrum of thiophene-2-carboxylicacid has been proposed by Sarswat et al. [20]. In the present study, the detailed interpretation of vibrational spectra, molecular interactions, and molecular docking studies on thiophene-2-carboxylicacid have been reported.

Experimental and computational details

The thiophene-2-carboxylic acid with a stated purity of 98% was purchased from Sigma Aldrich Company, India. The infrared spectrum of the sample was recorded on a BRUKER FT-IR instrument with a spectral resolution of 1.0 cm^{-1} in the region 400 to 4000 cm^{-1}. A KBr pellet of solid sample was prepared from the mixture of KBr and the sample in 200:1 ratio using hydraulic press. Multi-tasking OPUS software was used for signal averaging, signal enhancement, base line correction and other spectral manipulations. The FT-Raman spectrum was recorded using BRUKER RFS 27 stand alone FT-Raman spectrometer as powder sealed in a capillary tube in the region 0–4000 cm^{-1}. The line 1064 nm of Nd:YAG laser was used as an exciting source with an output power of about 100 mW at the sample position. Spectrum was accumulated for 100 scans with a resolution of 2 cm^{-1}.

The implementation of theoretical computations usually gives us supportive evidence to the experimental results. In this work, theoretical density functional method has been approached to find the single point energy, geometry optimization, potential energy scan, vibrational frequencies and second order perturbation energies of the title molecule. The entire calculations have been carried out using Gaussian 03W software package with the internally stored DFT/B3LYP/6-31+G(d,p) basis set [21–23]. For spectrum simulations and isodensity plots, visualization interface Gauss View 3.0 has been used [24]. The vibrational frequency assignments of this molecule were carried out using MOLVIB program package [25]. The interactions of TCA with certain protein structures which are responsible for inflammation have been analyzed docking simulation. In this work, docking simulations have been performed by SWISSDOCK webserver and the docking results were viewed with the help of UCSF Chimera visualization program [26,27].

Result and discussion

Energy minimization of Monomer

In the present work, single point energy for various possible conformers of the title molecule is determined and is given in Fig. S1 (Supplementary material). Stationary point on the potential energy surface has been found by varying dihedral angle (C_2—C_6—O_8—H_9) of the minimum energy conformer. It is also found that dihedral angle positioned at 180° gives local minima (E_{min} = −741.6049 Hartree) of the title molecule. The stationary point energy for the other dihedral angle positions and their relative energy with the stable conformer are given in Table S1 (Supplementary material). The potential energy surface scan along with structure corresponding to local minima is given in Fig. 1. The optimized geometrical parameters of minimum energy conformer of the title molecule are collected in Table 1. It is worth mentioning that the C—C bonds in the five member ring vary from 1.3756 Å to 1.4200 Å. Typically, the C—C bonds to the carbons adjacent to the sulfur are about 1.34 Å, the C—S bond length is around 1.70 Å, and the other C—C bond is about 1.41 Å for thiophene [28]. The substitution of carboxylic acid group in the ring produces diverse effect on both bond lengths and bond angles. In the title molecule, the C—C bonds to the carbons adjacent to the sulfur calculated at DFT/B3LYP with 6-31+G(d,p) basis set are about 1.3759 Å (C_4—C_5) and 1.38 Å (C_2—C_3). The C—S bond lengths are about 1.7253 Å (S_1—C_5) and 1.7429 Å (S_1—C_2), and the other C—C bond in the ring is about 1.42 Å.

On the other hand, when we look into the bond angles, we can find a variation of 2° in comparison with that of thiophene. For thiophene molecule, the bond angle at the sulfur is usually around 93°, the C—C—S angle is around 109° and the other two carbons have a bond angle around 114°. In the title molecule, the calculated

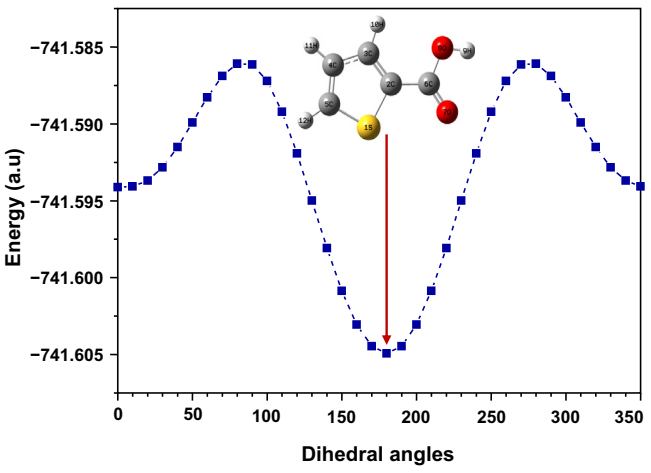

Fig. 1. Potential energy scan for the selected dihedral angle (C_2—C_6—O_8—H_9) of thiophene-2-carboxylicacid.

Table 1
Optimized geometrical parameters of thiophene-2-carboxylic acid obtained from theoretical DFT computations with B3LYP/6-31+G(d,p) method.

Parameters	Bond length (Å)	Parameters	Bond angle (°)	Parameters	Dihedral angle (°)
S1—C2	1.7429	C2—S1—C5	91.0	C5—S1—C2—C3	0.0
S1—C5	1.7253	S1—C2—C3	111.5	C5—S1—C2—C6	−180.0
C2—C3	1.3800	S1—C2—C6	119.6	C2—S1—C5—C4	0.0
C2—C6	1.4645	C3—C2—C6	128.9	C2—S1—C5—H12	−180.0
C3—C4	1.4200	C2—C3—C4	112.7	S1—C2—C3—C4	0.0
C3—H10	1.0831	C2—C3—H10	122.5	S1—C2—C3—H10	−180.0
C4—C5	1.3759	C4—C3—H10	124.8	C6—C2—C3—C4	180.0
C4—H11	1.0836	C3—C4—C5	112.3	C6—C2—C3—H10	0.0
C5—H12	1.0820	C3—C4—H11	124.2	S1—C2—C6—O7	0.0
C6—O7	1.2183	C5—C4—H11	123.5	S1—C2—C6—O8	180.0
C6—O8	1.3602	S1—C5—C4	112.5	C3—C2—C6—O7	180.0
O8—H9	0.9716	S1—C5—H12	119.8	C3—C2—C6—O8	0.0
		C4—C5—H12	127.7	C2—C3—C4—C5	0.0
		C2—C6—O7	125.2	C2—C3—C4—H11	−180.0
		C2—C6—O8	112.4	H10—C3—C4—C5	−180.0
		O7—C6—O8	122.4	H10—C3—C4—H11	0.0
		C6—O8—H9	106.5	C3—C4—C5—S1	0.0
				C3—C4—C5—H12	180.0
				H11—C4—C5—S1	180.0
				H11—C4—C5—H12	0.0
				C2—C6—O8—H9	180.0
				O7—C6—O8—H9	0.0

bond angle around sulfur atom is about 91°. Similarly, the calculated bond angles of C—C—S are about 111.5° (S1—C2—C3) and 112.5° (S1—C5—C4). It is also pointed out from Table 1 that the substitution of carboxylic acid group does not make much more effect on the dihedral angles of the title molecule.

Dimerization

The Fig. 2 presents the geometry of TCA dimer optimized at B3LYP/6-31+G(d,p) level using Gaussian 03W program package. The dimer entities in TCA can be proved by shaping the structure by joining high-frequency O—H stretching and low-frequency O···O stretching mode. The basic mechanism by coupling high-frequency O—H and low-frequency O···O band is known as anharmonic-type coupling [29]. The dimer structure shown in Fig. 2 contains two intermolecular hydrogen bonds which are similar as the model given by Boczar [29], Marechal and Witkowski [30]. The energy of the dimer structure calculated at B3LYP/6-31+G(d,p) is about (E = −1483.3941 a.u) and it is also found that, the energy of TCA dimer is found to be twice that of its stable monomer structure.

NBO analysis

To interpret the presence of intermolecular and intramolecular charge transfer interactions, the second order perturbation energies were calculated on both monomer and dimer conformer using B3LYP method with 6-31+G(d,p) combination in Gaussian 03W package. The second order perturbation energy is an utmost theoretical concept to estimate the delocalization of electron density between the principal occupied Lewis-type (bond or lone pair) orbitals and unoccupied non-Lewis (antibond or Rydberg) orbitals [31]. The electron occupancies of lone pair and anti-bonding orbitals of the title molecule are given in Table 2 and second order perturbation results are given in Table 3. The electron occupancies given in Table 2 shows the presence of non-bonded intramolecular interactions between lone pair LP(1) O7 and anti-bonding BD*(1) O8—H9 orbitals upon dimerization. In detail, the electron occupancy of lone pair orbital LP(1) O7 decreases by −0.07348 e (the negative sign indicates decrease in occupancy) when dimerize the stable monomer. In contrast, the electron occupancy of anti-bonding orbital BD*(1) O8—H9 increases by 0.06473 e. The occupancy and energy changes for the rest of other molecular orbitals are not significant. Hence we can say that predominant non-bonded interaction between O7 and O8—H9 leads to more chemical stability.

In the present work, the second order perturbation energies of most interacting Lewis base and Lewis acid sites are calculated using DFT computations with B3LYP/631+G(d,p) method. For each Lewis base (α) and Lewis acid (β), the stabilization energy, $E(2)$ associated with the delocalization $\alpha \rightarrow \beta$ is estimated as

$$E(2) = E(\beta) - E(\alpha) = q_\alpha \frac{F(\alpha,\beta)^2}{\varepsilon_\beta - \varepsilon_\alpha}$$

where q_α is the donor orbital occupancy, ε_α and ε_β are diagonal elements and $F(\alpha,\beta)$, the off diagonal NBO Fock matrix element.

Very large values of 36.96 and 36.91 kcal/mol were obtained due to the presence of intramolecular interactions between lone pairs LP (1) O7, LP (1) O16 and anti-bonding acceptors BD*(1) H13—O14, BD*(1) O8—H9, respectively. The results clearly depict the existence of intermolecular interactions as shown in Fig. 2. The second order perturbation energies within unit 1 and unit 2 show the presence of non-bonded weak intramolecular interactions in stable monomer geometry.

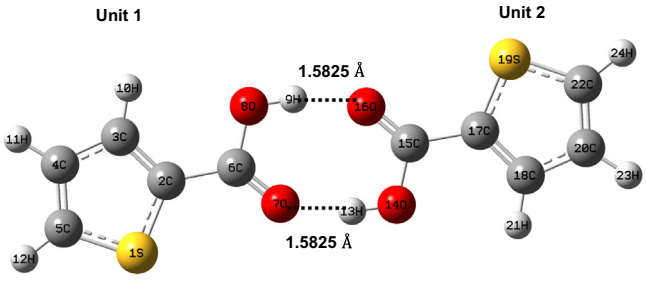

Fig. 2. Dimer structure of thiophene-2-carboxylicacid.

Vibrational frequency assignments

The vibrational frequency calculations made in this study reveals that the title molecule belongs to C1 point group symmetry

Table 2
Occupancies and energies of most interacting Lewis base and Lewis acid sites of monomer and dimer conformer of thiophene-2-carboxylicacid.

Parameters	Occupancies (e)		Δ_{Occ} (e)	Energy (ev)		Δ_E (eV)
	Monomer	Dimer		Monomer	Dimer	
LP(1) S1	1.98153	1.98007	−0.00146	−0.64213	−0.65312	−0.01099
LP(1) O7	1.97987	1.90639	−0.07348	−0.72221	−0.56486	0.15735
LP(1) O8	1.97771	1.96923	−0.00848	−0.62098	−0.54945	0.07153
BD*(1) S1—C2	0.02315	0.02191	−0.00124	0.25652	0.25286	−0.00366
BD*(1) S1—C5	0.01531	0.01420	−0.00111	0.25597	0.25751	0.00154
BD*(1) C2—C3	0.01805	0.01873	0.00068	0.56683	0.55911	−0.00772
BD*(1) C2—C6	0.07156	0.06955	−0.00201	0.33719	0.33732	0.00013
BD*(1) C3—C4	0.01371	0.01260	−0.00111	0.50387	0.50235	−0.00152
BD*(1) C3—H10	0.01396	0.01353	−0.00043	0.45248	0.48911	0.03663
BD*(1) C4—C5	0.01493	0.01648	0.00155	0.56041	0.55379	−0.00662
BD*(1) C4—H11	0.01446	0.01353	−0.00093	0.44891	0.48155	0.03264
BD*(1) C5—H12	0.01298	0.01198	−0.00100	0.43605	0.46921	0.03316
BD*(1) C6—O7	0.01720	0.02518	0.00798	0.55662	0.55920	0.00258
BD*(1) C6—O8	0.08993	0.07546	−0.01447	0.32236	0.33770	0.01534
BD*(1) O8—H9	0.00989	0.07462	0.06473	0.37250	0.51125	0.13875

Table 3
Second order perturbation energies of most interacting NBO's of thiophene-2-carboxylicacid.

Lewis base (α)	Lewis acid (β)	$E(2)$ (kcal/mol)	E(β) − E(α) (a.u)	$F(\alpha,\beta)$ (a.u)
Within unit 1				
LP(1) S1	BD*(1) C2—C3	3.24	1.21	0.056
LP(1) S1	BD*(1) C4—C5	2.55	1.21	0.050
LP(1) O7	BD*(1) C6—O7	0.71	1.12	0.026
LP(1) O7	BD*(1) C6—O8	10.57	0.90	0.088
LP(1) O8	BD*(1) C2—C6	0.85	0.89	0.025
LP(1) O8	BD*(1) C6—O7	7.97	1.11	0.084
From unit 1 to unit 2				
LP (1) O7	BD*(1) H13—O14	36.96	1.13	0.183
From unit 2 to unit 1				
LP (1) O16	BD*(1) O8—H9	36.91	1.12	0.181
Within unit 2				
LP (1) O14	BD*(1) C15—O16	8.30	1.09	0.085
LP (1) O16	BD*(1) O14—C15	4.95	1.00	0.063
LP (1) S19	BD*(1) C17—C18	3.28	1.21	0.056
LP (1) S19	BD*(1) C20—C22	2.62	1.21	0.050

and it has 30 vibrational normal modes of same symmetry species. The possible internal coordinates and non-redundant set of symmetry coordinates for the title molecule have been collected in Tables S2 and S3 (Supplementary material), respectively. The percentage of potential energy distribution (PED) obtained from MOLVIB program package is used for assigning vibrational peaks. The exclusion of anharmonicity factor and the level of basis set used, the theoretical frequencies are not matched with that of the experimental. Hence linear scaling procedure is adopted to scale down the frequency values. The experimental FT-IR, FT-Raman and theoretical scaled wavenumbers along with IR, Raman intensities and their corresponding vibrational assignments are given in Table 4. The experimental FT-IR spectrum is shown in Fig. 3 and theoretical scaled IR and Raman spectra are given in Fig. 4. The detailed interpretations of functional group vibrations are summarized as follows;

Ring vibrations

In the present study, the ring stretching vibration is observed as medium intensity peak at 1406 cm^{-1} in FT-IR spectrum. Sarswat et al. reported ring stretching vibration as strong intensity peak at 1412 cm^{-1} in FT-Raman spectrum [20]. The theoretical wavenumber corresponding to this mode scaled down by 0.956 is in excellent agreement with experimental one. Due to the absence of peaks for ring in-plane and out-of-plane vibrations, the theoretically scaled values at 994, 610 and 562 cm^{-1} are assigned to ring in-plane vibrations and at 430, 168 and 162 cm^{-1} are assigned to ring out-of-plane vibrations on the basis of PED percentage. In the title molecule, the stretching vibrations of C—S are calculated at 830 and 698 cm^{-1} by B3LYP/6-31+G(d,p).

C—H vibrations

Usually thiophenes and its derivatives produce peaks in the region 3120–3100 cm^{-1} due to C—H stretching vibration [32]. In the present study, the peaks observed at 3113, 3098 and 3082 cm^{-1} in FT-IR spectrum are assigned to C—H stretching vibrations. Theoretically scaled values of 3118, 3102 and 3084 cm^{-1} at B3LYP/6-31+G(d,p) are in good agreement with the experimental FT-IR. The PED results indicate that they are very pure modes.

Thiophenes also have bands of variable intensity in the region 1550–1200 cm^{-1} due to C—H in-plane vibrations [32]. For TCA, the peaks identified at 1311 cm^{-1} in FT-IR and at 1353 cm^{-1} in FT-Raman are ascribed to C—H in-plane bending modes. PED results show that these modes are strongly influenced by ring stretching (υC—C, υC—S) and OH in-plane bending (βOH) vibrations.

Mono substituted thiophenes have two bands of medium to strong intensity band at 745–695 cm^{-1} and the other at 700–660 cm^{-1} possibly due to out-of-plane binding of =C—H group [33]. In the title molecule, the peaks identified at 725 and 664 cm^{-1} in FT-IR and 721 cm^{-1} in FT-Raman are attributed to C—H out-of-plane bending vibrations.

Table 4
Vibrational frequency assignments of thiophene-2-carboxylicacid.

Experimental wavenumbers		Calculated wavenumbers		IR intensity	Raman intensity	Vibrational assignments[b]
IR	Raman[a]	Unscaled frequency	Scaled frequency			
–	–	79	76	0.1	0.1	τCOOH(65), γRing(30)
–	–	170	162	0.3	1.0	γRing(84)
–	–	175	168	0.5	0.1	γRing(79)
–	–	373	357	1.4	1.7	βCOOH(50), βRing(28)
–	428 vw	450	430	2.8	0.5	γCS(48), γCH(26), γOH(19)
–	455 w	464	444	0.2	1.2	βRing(58)
515 ms	519 ms	548	524	12.4	0.5	γC—COOH(65),γCH(20)
–	–	588	562	8.4	1.2	γCC(53), γOH(31)
–	–	639	610	7.5	2.1	βCS(48), βCOOH(21)
664 s	–	708	677	7.2	14.2	βRing(62)
–	–	730	698	13.4	0.4	γCH(96)
725 w	721 w	756	723	0.9	2.7	γCH(92)
738 w	741 s	761	728	13.9	0.1	βCC(49), βCH(25), γOH(14)
–	–	868	830	0.4	0.3	υCS(77)
–	–	869	831	4.1	3.0	υCS(72)
–	–	931	890	0.1	0.4	γCH(94)
–	–	1040	994	15.5	1.2	βRing(48), υCC_{out}(17)
1046 m	1050 w	1088	1041	21.7	3.2	υC—O(45), βCH(22)
1078 s	1078 s	1112	1063	7.9	8.6	υCC_{out}(43), βCH(21)
–	–	1205	1152	47.1	10.2	βOH(59), υCC_{out}(18)
–	–	1258	1203	0.1	1.8	υCC(60), υCS(28)
1311 ms	–	1366	1306	20.7	2.7	βCH(53), βOH(22), υCC_{out}(15)
–	1353 s	1396	1334	8.0	7.2	βCH(61), υCC(18), βOH(13)
1406 ms	1412 vs	1468	1403	22.1	96.1	υCC(56), βCH(28)
–	–	1570	1501	6.2	3.8	υCC(62), βCH(30)
1690 vw	–	1779	1701	100.0	69.0	υC=O(76)
3082 s	–	3226	3084	0.9	62.2	υCH_{as}(94)
3098 m	–	3245	3102	0.1	58.7	υCH_{as}(96)
3113 ms	–	3262	3118	0.1	100.0	υ_{ss}CH(95)
–	–	3767	3601	23.5	79.6	υOH(100)

[a] FT-Raman peak values are taken from the Ref. [31].
[b] υ – stretching, β – in-plane bending, γ – out-of-plane bending, τ – Torsion.

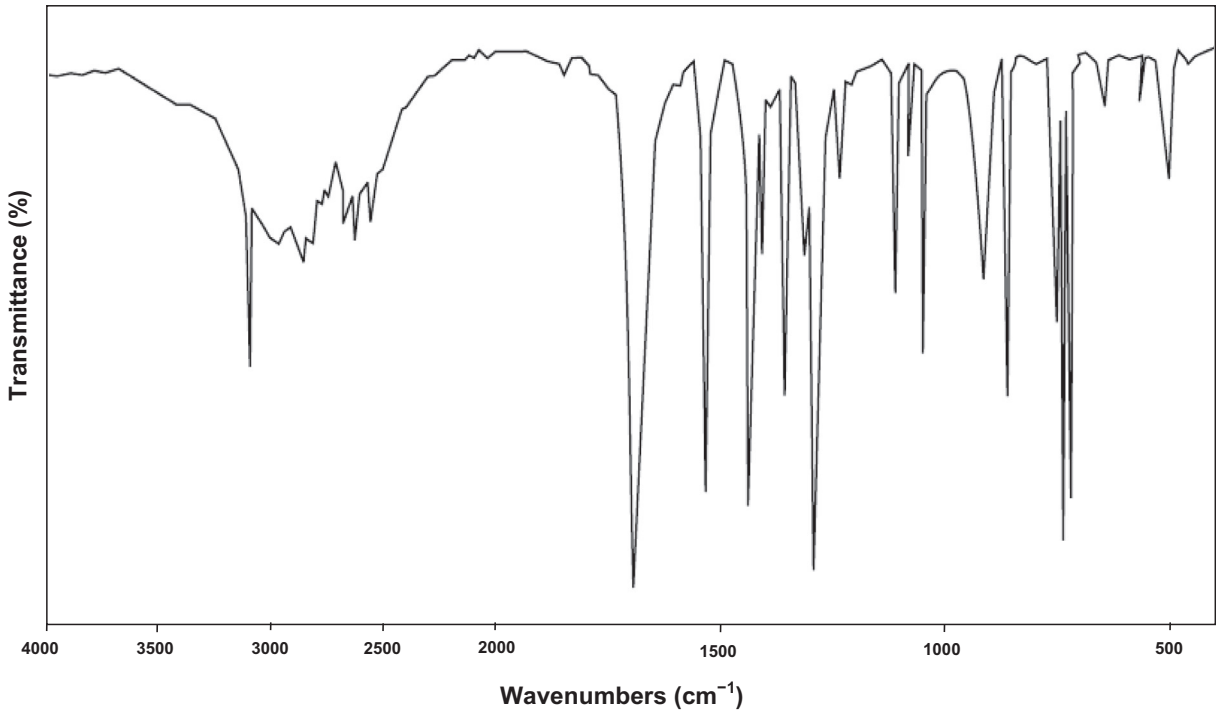

Fig. 3. Experimental FT-IR spectrum of thiophene-2-carboxylic acid.

C—COOH vibrations

The carbon atom of the —COOH group linked with thiophene ring produces three distinct vibrations of medium to strong intensity in the region 500–1100 cm^{-1} of FT-IR spectrum shown in Fig. 3. The C—C stretching vibration of this group generates a strong intensity peak at 1078 cm^{-1} in FT-IR and FT-Raman. A medium intensity peak at 515 cm^{-1} in FT-IR and at 519 cm^{-1} in FT-Raman spectrum is assigned to C—C out-of-plane bending

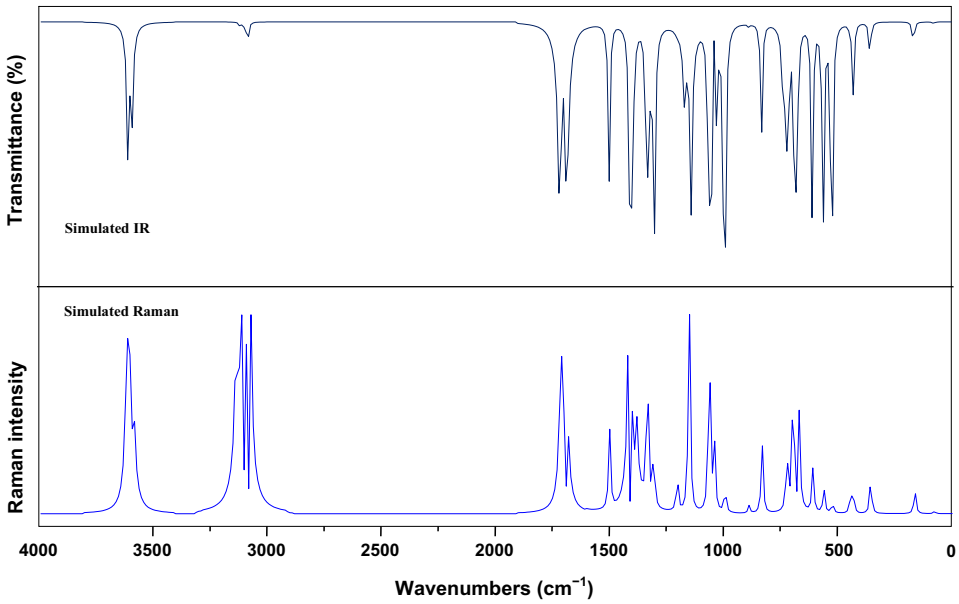

Fig. 4. Simulated IR and Raman spectra of thiophene-2-carboxylic acid.

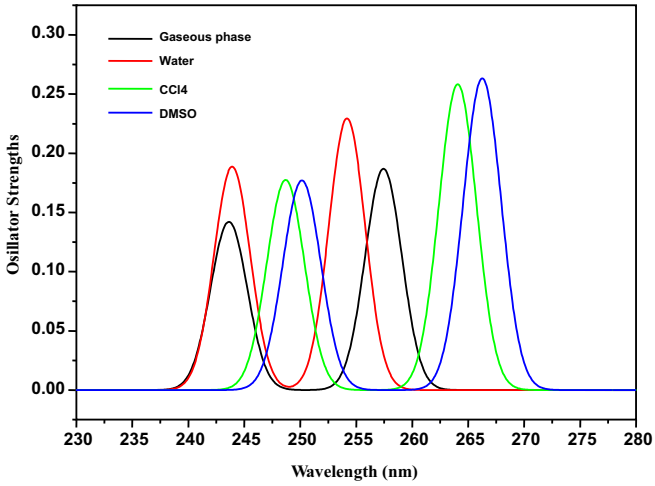

Fig. 5. Theoretical UV spectra of thiophene-2-carboxylic acid in different solvents.

vibration. The stretching vibration of OH is not active in IR spectrum. Hence theoretically scaled value at 3601 cm^{-1} is assigned to this mode on the basis of PED percentage. The stretching vibration of C═O is always considered to be characteristic frequency for carboxylic acids. A very sharp and medium intensity peak at 1690 cm^{-1} in FT-IR spectrum is assigned to C═O stretching vibration. The assignment of this mode is in excellent correlation with that of similar kind of molecule [16]. On the other hand, C—O stretching vibration is identified at 1046 cm^{-1} in FT-IR and 1050 cm^{-1} in FT-Raman spectrum. The in-plane and out-of-plane vibrations of —COOH group are only possible to appear in Far IR region. Hence these peaks are assigned on the basis of PED results.

UV–Vis spectra

In order to investigate the electron transition between the energy levels, the singlet–singlet allowed spin states are to be considered [34]. In the present study, the maximum absorption wavelengths (λ_{max}), Excitation energies (ΔE), and oscillator strength of TCA with different solvents are calculated using TD-DFT/B3LYP method with 6-31G+(d,p) basis set combination. The theoretical UV–Vis spectra of TCA in gaseous phase and in various solvents are given in Fig. 5. In the gaseous phase, the λ_{max} corresponding to the excitation of one electron transition from HOMO (highest occupied molecular orbitals) to LUMO (lowest occupied molecular orbitals) is calculated at 259.69 nm with negligible oscillator strength. The reduced excitation energies found in the solvents CCl4 and DMSO result in its increased conductivity and they produce peaks at 264.07 nm and 266.26 nm, respectively. In the case of TCA in water solvent, the reduced λ_{max} value increases the gap between HOMO and LUMO according to the relation ($\lambda = \frac{hc}{E}$) leads to decreased conductivity. The λ_{max} values corresponding to HOMO-1 to LUMO and HOMO-2 to LUMO state transitions along with their oscillator strengths and excitation energies are given in Table 5. For this solvent effect determination, the polarisable continuum model (PCM) is used [35]. The UV–Vis spectra of a molecule in different solvents are given in Fig. 5. The transitions observed in this case are belonging to $\pi \rightarrow \pi^*$ type. In general,

Table 5
Theoretical maximum absorption wavelengths (λ_{max}), excitation energies (ΔE) and oscillator strengths (f) of thiophene-2-carboxylicacid in gas phase and in different solvents by B3LYP/6-31+G(d,p) method.

Excitation states	Gaseous phase			Water phase			CCL4			DMSO			Transition type
	λ_{max} (nm)	f	ΔE (eV)	λ_{max} (nm)	f	ΔE (eV)	λ_{max} (nm)	f	ΔE (eV)	λ_{max} (nm)	f	ΔE (eV)	
H → L	259.69	0.0000	4.7744	254.18	0.2295	4.8779	264.07	0.2583	4.6951	266.26	0.2633	4.6565	$\pi \rightarrow \pi^*$
H-1 → L	257.44	0.1869	4.8161	246.07	0.0000	5.0385	254.66	0.0000	4.8686	250.15	0.1770	4.9563	$\pi \rightarrow \pi^*$
H-2 → L	243.63	0.1421	5.0891	243.92	0.1887	5.0830	248.70	0.1775	4.9853	249.31	0.0000	4.9731	$\pi \rightarrow \pi^*$

Table 6
Full fitness score, binding affinity and hydrogen bond interactions of TCA against various protein targets.

Ligand	PDB code for targets	Target chain	Full fitness score (kcal/mol)	Binding affinity (kcal/mol)	Hydrogen bond lengths (Å)
TCA	1PTH	A	−2181.83	−6.28	2.062 3.794 4.106
		B	−2181.83	−6.28	2.062 3.793 4.100
TCA	1CX2	A	−2499.89	−6.15	1.822 2.149 4.043 4.534
		B	−2493.86	−6.13	1.828 2.153 3.965 4.050
		C	−2499.60	−6.12	1.827 2.126 4.081 4.309
		D	−2492.07	−6.12	1.827 2.146 4.012 4.297

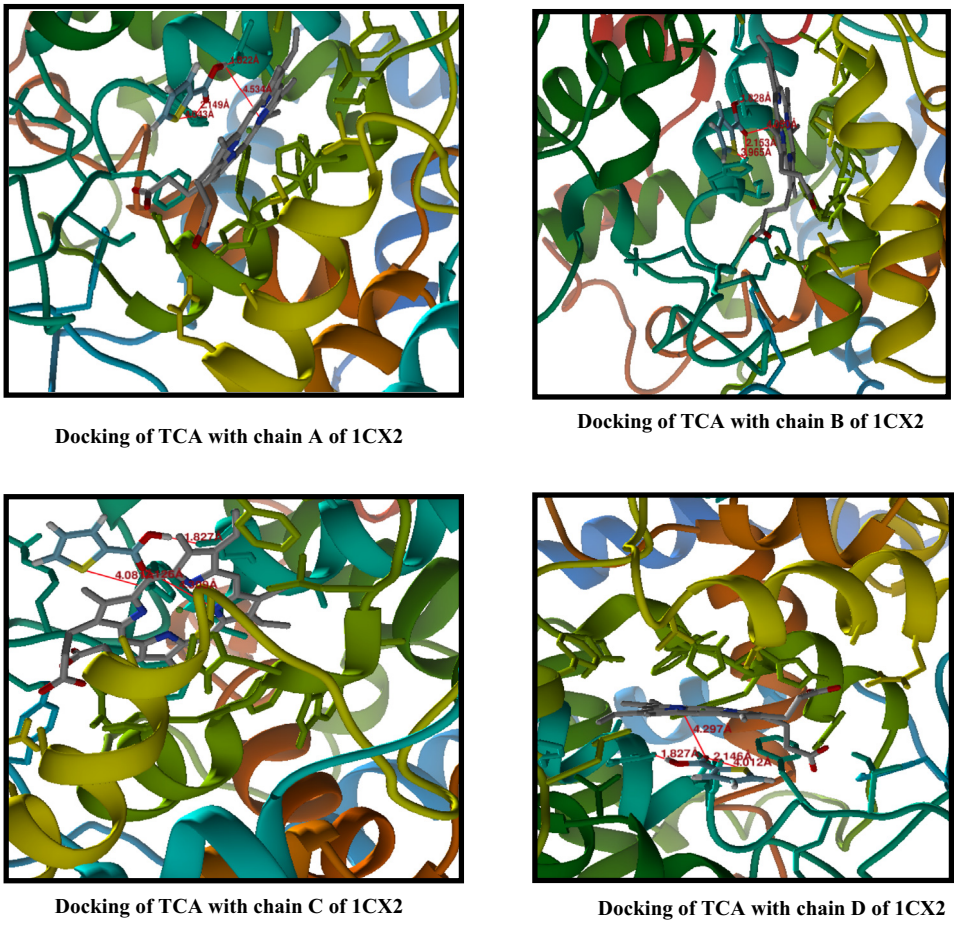

Fig. 6. Hydrogen bond interactions of TCA with 1CX2 protein structure.

the position of $\pi \rightarrow \pi^*$ transition in carbonyl compounds vary with the nature of the solvent used. As expected, the energy gap between π and π^* level of the title molecule decreases and the $\pi \rightarrow \pi^*$ transition undergo a bathochromic shift [36].

Binding affinity from molecular docking studies

The title molecule has wide scope in the medicinal field as an inhibitor drug for many diseases. To test the biological anti-inflam-

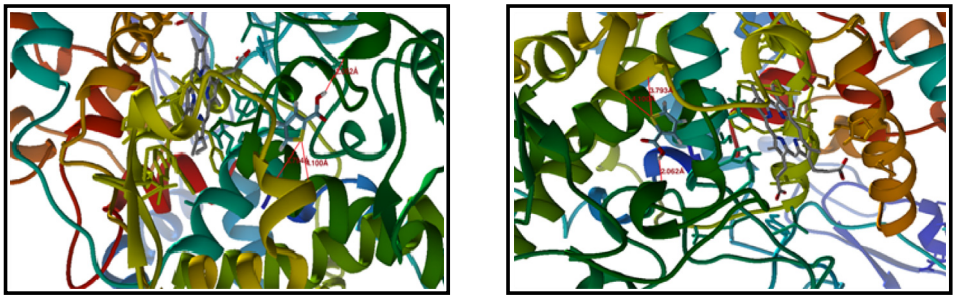

Fig. 7. Hydrogen bond interactions of TCA with 1PTH protein structure.

mation activity of TCA against Cyclooxygenesh-2 (Protein Data Bank Code: 1CX2), Prostaglandin H2 synthase (Protein Data Bank Code: 1PTH) and anti-immuno deficiency activity against HIV-1 protease with KNI-272 (Protein Data Bank Code: 1HPX), molecular docking studies have been performed using SWISSDOCK webserver [25]. Prior to performing molecular docking, the protein data bank (PDB) files were prepared using Dock prep tool available in free software package UCSF chimera [26]. In order to avoid sampling bias, docking runs were performed as blind by covering the entire protein and not defining any specific region of the protein as bonding pocket. Output clusters were obtained after each run and the results showed that cluster 0 is having the best full fitness (FF) score.

A greater negative FF scores for each protein chains are given in Table 6 along with their binding affinity against TCA and hydrogen bond distances. A greater negative FF score indicates a more favorable binding mode with a better fit. The FF score values obtained for protein targets clearly show that the TCA has bonded effectively with 1CX2 target sites with four notable hydrogen bonds. Out of these, side chain A of 1CX2 is strongly bind with TCA by hydrogen bonds 1.822 Å, 2.149 Å, 4.043 Å, and 4.534 Å. The docking picture obtained from UCSF chimera for TCA against 1CX2 and 1PTH targets are given in Figs. 6 and 7, respectively. Similarly, the best full fitness score for TCA against 1PTH clearly indicates its effective binding fit. From the results we can say that the TCA molecule is highly bonded with active residues of 1CX2 and 1PTH by hydrogen bond interactions leads to more anti-inflammatory activity. National cancer institute at USA has done few studies with 1CX2 proteins. They showed that 1CX2 inhibitor has been shown to reduce the occurrence of cancer and cancerous growths. Hence TCA can also be used as an inhibitor for cancerous diseases.

Conclusion

The title molecule under investigation has wide biological applications. Hence, spectroscopic investigation along with quantum chemical computations has been performed to show its spectroscopic signature, charge transfer interactions and biological activity. According to peak observed and PED result all the vibrational normal modes have been assigned carefully. The natural bond orbital analysis performed in this study gives information about the molecular species which are responsible for more chemical stability. The theoretical UV spectra of TCA in different solvents has been simulated by using PCM model with TD-DFT/B3LYP/6-31+G(d,p) basis set combination. The maximum absorption wavelengths and their excitation energies predicted in this study belong to $\pi \rightarrow \pi^*$ type. Moreover, molecular docking simulations have been done to test the biological inhibition activity against inflammation. The results showed that TCA molecule has potential activity against inflammation.

Acknowledgement

We would like to thank Mr. Salam pradeep singh, Ph.D scholar, Department of Molecular Biology and Biotechnology at Tezpur university, Assam, India and Mr. Renukesh Verma, Researcher at Madhav Institute of Technology and Science, India for their help during docking simulations.

Appendix A. Supplementary data

Supplementary data associated with this article can be found, in the online version, at http://dx.doi.org/10.1016/j.saa.2015.01.025.

References

[1] V.S. Sajia, K. Zong, M. Pyoa, J. Photochem. Photobiol., A 212 (2–3) (2010) 81–87.
[2] <http://www.chemicalland21.com/lifescience/phar/THIOPHENE-2-CARBOXYLIC%20ACID.htm>.
[3] L. Chan, O. Pereira, T.J. Reddy, S.K. Das, C. Poisson, et al., Bioorg. Med. Chem. Lett. 14 (2004) 793–796.
[4] L. Chan, O. Pereira, T.J. Reddy, S.K. Das, C. Poisson, et al., Bioorg. Med. Chem. Lett. 14 (2004) 797–800.
[5] A. Pinelli, A. Capuano, M. Bellei, Naunyn-Schmiedeberg's Arch. Pharmacol. 279 (1973) 203–206.
[6] G. Babu, H.M. Yu, S.M. Yang, J.M. Fang, Bioorg. Med. Chem. Lett. 14 (2004) 1129–1132.
[7] H. Deng, J. Hu, H. Hu, M. He, Y. Fang, Bioorg. Med. Chem. Lett. 22 (2012) 4148–4152.
[8] A.E. MacKenzie, J.E. Lappin, D.L. Taylor, S.A. Nicklin, G. Milligan, Front. Endocrinol. 2 (2011) 1–10.
[9] H. Deng, H. Hu, S. Ling, A.M. Ferrie, Y. Fang, ACS Med. Chem. Lett. 3 (2012) 165.
[10] K. Pasterny, R. Wrzalik, T. Kupka, G. Pasterna, J. Mol. Struct. 614 (1–3) (2000) 297–304.
[11] V. Hernández, F.J. Ramírez, J. Casado, F. Enríquez, J.J. Quirante, J.T.L. Navarrete, J. Mol. Struct. 410–411 (1997) 311–314.
[12] T. Kupka, R. Wrzalik, G. Pasterna, K. Pasterny, J. Mol. Struct. 616 (1–3) (2002) 17–32.
[13] G.D. Fleming, R. Koch, M.M.C. Vallete, Spectrochim. Acta 65A (3–4) (2006) 935–945.
[14] D.K. Singh, S.K. Srivastava, A.K. Ojha, B.P. Asthana, J. Mol. Struct. 892 (1–3) (2008) 384–391.
[15] L.X. Hong, L.X. Ru, Z.X. Zhou, Comput, Theor. Chem. 969 (1–3) (2011) 27–34.
[16] V. Balachandran, A. Janaki, A. Nataraj, Spectrochim. Acta 118A (2014) 321–330.
[17] L.L. Gladkov, S.V. Gaponenko, E.V. Shabunya-Klyachkovskaya, A.N. Shimko, E.S. Al-Abdullah, A.A. El-Emam, Spectrochim. Acta 128A (2014) 874–879.
[18] S. Abbas, M. Hussain, S. Ali, M. Parvez, A. Raza, A. Haider, J. Iqbal, J. Organomet. Chem. 724 (2013) 255–261.
[19] T. Nasr, S. Bondock, S. Eid, Eur. J. Med. Chem. 84 (2014) 491–504.
[20] P.K. Sarswat, A. Sathyapalan, Y. Zhu, M.L. Free, J. Theor. Appl. Phys. 7 (1) (2013) 1–9.
[21] M.J. Frisch, G.W. Trucks, H.B. Schlegel, G.E. Scuseria, et al., Gaussian 03, Revision B.01, Gaussian Inc., Pittsburgh, PA, 2003.
[22] A.D. Becke, J. Chem. Phys. 98 (1993) 5648–5652.
[23] C. Lee, W. Yang, G.R. Parr, Phys. Rev. B 37 (1998) 785–789.
[24] A.E. Frisch, R.D. Dennington, T.A. Keith, A.B. Neilsen, A.J. Holder, Gauss View 3.0, Gaussian Inc., Pittsburgh, PA, 2003.
[25] T. Sundius, MOLVIB: a program for harmonic force field calculations, QCPE program no. 604, 1991.
[26] A. Grosdidier, V. Zoete, O. Michielin, Nucleic Acids Res. 39 (2011) W270–W277.

[27] E.F. Pettersen, T.D. Goddard, C.C. Huang, G.S. Couch, D.M. Greenblatt, E.C. Meng, T.E. Ferrin, J. Comput. Chem. 13 (2004) 1605–1612.
[28] Cambridge crystallography data base.
[29] M. Boczar, L. Boda, M.J. Wojcik, Spectrochim. Acta 64A (2006) 757–760.
[30] Y. Marechal, A. Witkowski, J. Chem. Phys. 48 (1968) 3697.
[31] T. Karthick, V. Balachandran, S. Perumal, A. Nataraj, Spectrochim. Acta 107A (2013) 72–81.
[32] M. Rico, J.M. Orza, J. Morcilla, Spectrochim. Acta 21 (1965) 689–719.
[33] A. Hidalgo, J. Phys. Radium 16 (1955) 366–372.
[34] V. Balachandran, T. Karthick, S. Perumal, A. Nataraj, Indian J. Pure Appl. Phys. 51 (2013) 178–184.
[35] B. Mennucci et al., J. Phys. Chem. A 106 (2002) 6102–6113.
[36] J. Mohan, Organic Spectroscopy: Principles and Applications, second ed., Narosa Publishing House, New Delhi, 2011.